Experiments in Fluids 22 (1996) 165–173 © Springer-Verlag 1996

Reduction of beam refraction in optical pipe flow experiments by use of sheet-fabricated pipe walls

W. Steenbergen

Abstract A measurement section is presented that allows for the study of liquid flows in straight pipes with noninvasive optical techniques. The amount of refraction of light rays is minimized by the use of short pipe sections manufactured of transparent film. For the situation of water, it is shown that walls as thin as 85 μm can be used in turbulent flows at high velocities. In our specific case, a flow of water at Reynolds numbers upto $Re_D = 300\,000$ in a pipe of ∅ 70 mm diameter (average velocity 4 m/s) was realized without unacceptable vibrations of the pipe wall. In this situation laser Doppler measurements can be carried out without the need to correct for the position of the measurement volume or changes in the velocity response of the system.

1 Introduction

Due to its fundamental nature, pipe flow is still of considerable importance in fluid dynamics research. Many industrial processes of mass and heat transport or chemical reaction take place in pipes, which explains the practical relevance of this geometry. Since pipe flows have been studied extensively, they are particularly appropriate for the evaluation of new experimental techniques, since the velocity distributions to be expected in fully developed flows, either turbulent or laminar, are well documented, see e.g. Schlichting (1979) and Hinze (1975).

An evident complication in the study of pipe flows with noninvasive optical techniques is the curvature of the pipe wall. Without precautions, this leads to distorted images in the case of image-based techniques, and positioning and interpretation errors in the case of laser Doppler velocimetry (LDV). In principle, some refraction effects may be restored by an inverse application of Snell's law to the optical situation at hand. Examples of such correction procedures are given by Boadway and Karahan (1981) for the case of LDV, and by Lowe and Kutt (1992) for image reconstruction. However, apart from traceable errors, refraction may impede measurements in certain regions due to total internal reflection. Furthermore, if due to refraction the laser beams fail to occupy a common volume, the application of LDV may be inhibited even in regions where the absolute amount of refraction is small.

To minimize or prevent the problems related to the refraction of the beams by the pipe wall, a number of precautions may be taken.

Immersion in a square box By mounting the transparent pipe in a liquid-filled box with flat windows, the largest optical transition, *viz.* that between air and the liquid, is made flat. This is a standard measure, which always should be taken even in combination with one of the following specific measures.

Refractive index matching In fluid flows, it may be possible to control the index of refraction of the fluid. By making the refractive indices of the transparent pipe and the fluid equal, refraction is eliminated. Examples of this practice are given by Dybbs and Edwards (1987), who used various mixtures of two types of oils. Refractive index matching is generally limited to small flow rigs due to the cost of these fluids, the necessity of temperature control and the possible change of the optical properties due to ageing. Furthermore, it may be necessary to seal the systems, since fluids proper for refractive index matching are often volatile and noxious. A disadvantage from the fluid mechanical point of view is the relatively high kinematic viscosity of these fluids relative to standard fluids like water.

Corrective lenses It is possible to anticipate for the effect of refraction by the use of corrective lenses that deflect the laser beams before they enter the flow system. An example of this approach is the work of Ritterbach et al. (1987), who propose the use of simple spherical lenses. The general disadvantage of such strategies is, that each optical situation requires a specific lens geometry. Often, rather complicated lenses are required. Furthermore, it may be necessary to realign the lenses between two measurement positions. Even when a complete correction

Received: *15 February 1996*/*Accepted*: *21 May 1996*

W. Steenbergen
Eindhoven University of Technology,
Faculty of Applied Physics, Fluid Dynamics Laboratory.
PO Box 513, NL 5600 MB Eindhoven, The Netherlands

Current address:
University of Twente, Faculty of Applied Physics,
Applied Optics Group, PO Box 217, NL 7500 AE, Enschede,
The Netherlands.

The author is indebted to Johan Stouthart, who provided indispensible support during the design of the measurement section and the measurements.
Dantec Nederland is acknowledged for the loan of a 55X vibrometer system. This research was partly sponsored by *NV Nederlandse Gasunie* (The Netherlands), *BV Nederlandse Aardolie Maatschappij* (The Netherlands) and *Ruhrgas AG* (Germany).

for the measurement position is obtained, the beam intersection angle will vary from point to point, which further complicates the measurement procedure.

Thin pipe walls It is obvious that a reduction of the pipe wall thickness leads to a smaller amount of refraction, provided that the pipe is surrounded by a rectangular box as described above. Although it is possible to manufacture pipe sections with a wall thickness smaller than 100 μm out of a thicker pipe, it is difficult to obtain a satisfactory optical quality in this way. A better result is obtained by the use of prefabricated flexible transparent films. Mizushina and Usui (1977) used short pipe sections made of polyester film with a thickness of 35 μm and an internal diameter of 2.53 cm. Their test fluid was water with a dilute polyethylene oxide solution. Van Maanen and Fortuin (1983) removed a half part of a ∅ 50 mm glass pipe over a length of 16 cm, while the complete inner wall of the pipe was covered with a thin transparent film (type unreported) with a thickness of 100 μm. In this way they were able to perform LDV measurements of water flow at a distance as small as 0.5 mm from the wall with the bisector of the laser beams parallel to the wall. A third example is the work of Kunen (1984), who used an acetate film of 100 μm thickness, for a pipe with a diameter of 44 mm, filled with water. In these references, no attention is given to the complications encountered with transparent films, like motions generated by turbulent pressure fluctuations, the optical behaviour of films, the technical setup of the test-section and handling procedures, the selection of sheet material, etc. The purpose of the present article is to give the reader an impression of the practical possibilities and limitations of the method.

2 Design of the test section

For a liquid-filled pipe with a perfectly circular shape which is surrounded by a completely closed vessel filled with the same liquid, it is *in principle* impossible to change its cross-sectional shape, even when the pipe wall is flexible. Any motion of the pipe wall, either in an axisymmetric or an asymmetric mode, would change the volume of the liquid in the surrounding vessel, which is impossible due to the incompressibility of the liquid. This, however, is mere theory since a perfectly circular shape will never be obtained. Furthermore, this reasoning is based on the assumption that the fluid compartments inside and outside the pipe are completely separated, a situation which is difficult to realize in practice. There may always be some leakage along the edges of the film, even when it is glued or sealed with "o"-rings. This might result in an instability when a part of the flexible pipe wall is convex in the mean flow direction: the resulting local underpressure will tend to increase the wall curvature, and eventually the film collapses. This may be prevented by keeping the pressure of the surrounding fluid slightly below the local pressure inside the pipe. The most controlled manner is to make a pressure connection between the surrounding fluid and a point downstream of the flexible pipe section.

The test section presented in this article is used for LDV measurements in water, in a test pipe with a diameter of 70 mm and a length of 21 m. The optical measurement section may be used at any station within this test pipe, and should allow for measurements in planes with an axial separation of one pipe diameter. The test pipe is included in a gravity-driven closed test circuit. Typical velocities to be realized are 4–5 m/s. The test section should give a maximum optical access to the pipe, hence with a minimum of obstructions.

Figure 1 gives a schematic impression of the way in which such a pipe section is integrated in the pipe, while Fig. 2 shows the total test section, including three optical measurement ports. These ports are placed at one, three and five diameters distance of one connection, and two, four and six diameters distance from the other end. Hence, the section allows for measurements with a streamwise resolution of one pipe diameter. The pipe sections are made of polyester sheet (standard write on overhead transparency, copyproof transparencies are too hazy) with a thickness of 85 μm. It is glued into a cylindrical shape by means of a glue strip, item 1 in Fig. 1. Both open ends are reinforced with brass rings (3) of 1 mm thickness.

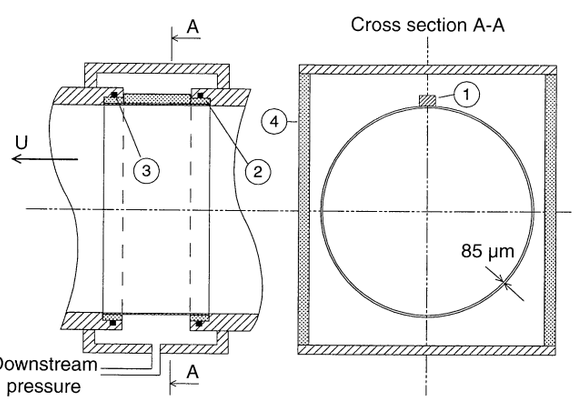

Fig. 1. LDV measurement section (not to scale) in two cross-sections. The boldface arrow indicates the flow direction

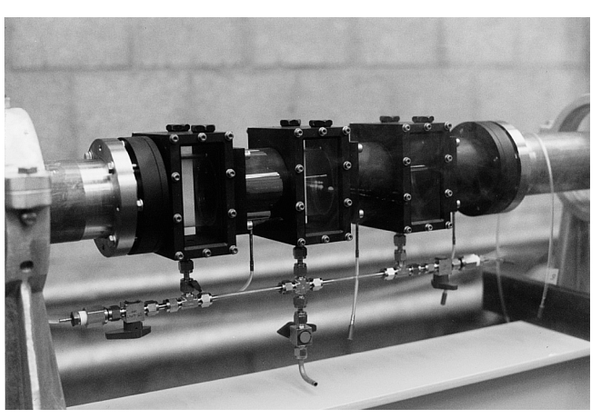

Fig. 2. The optical measurement section, consisting of three units such as shown in Fig. 1. The black part can be rotated about the pipe axis

The three vessels surrounding the transparent pipe sections are linked to a point approx. 1 m downstream of the test-section by means of flexible thin plastic tubing. The pressure difference over the sheet appeared to be sufficiently large to make the pipe section stable and round.

The connections between the measurement section and the upstream and downstream pipes are designed such that the measurement section may be rotated during an experiment. This yields flexibility in the choice of measurement trajectories and velocity components to be measured with LDV.

3
Handling of the test section

The fragility of the transparent pipes requires a careful handling during their insertion into the test pipe, and during the operation of the complete pipe circuit. During the insertion of the transparent pipes into the "o" ring-containing chambers, they should be internally supported by a narrowly fitting smooth cylinder. Also critical are the procedures for filling and draining the system. During the filling, the water levels inside the test pipe and inside the rectangular vessels should be kept more or less equal. Special care is required to prevent air bubbles to remain in the rectangular vessels. Large air bubbles were removed by means of a thin tube connected to a syringe. When the system is filled with tap water, often small air bubbles (<1 mm) will appear. After the system is pressurized, these air bubbles dissolve within a few hours.

During the draining procedure, sudden internal pressure changes should be avoided when the water level has dropped below the level of the test pipe, since the transparent pipes may collapse. This happened several times due to the sudden release of large air bubbles trapped in the lower part of the pipe system. It may be avoided by connecting both the rectangular vessels and the interior of the test pipe to the laboratory room by means of sufficiently large connections, by which pressure differences over the transparent sheet are impeded.

The system should be started slowly enough to let the under-pressure originating down-stream the pipe propagate to the fluid surrounding the transparent pipes.

4
Fluid induced motion of the transparent pipes

An important matter is the occurrence of fluid-induced motions of the transparent pipe wall, in particular when near-wall measurements are to be performed. At several flow velocities, the motion of the pipe wall was measured with a *Dantec 55X Vibrometer*, see Buchhave (1975). This instrument is generally used to measure the velocity of vibrating objects. A single laser beam illuminates a spot of the vibrating target. The Doppler- shift ω_D of the backscattered light contains information of the velocity component V parallel to the beam, according to the Doppler equation

$$\omega_D = \frac{2n_f}{\lambda_0} V \tag{1}$$

with n_f the index of refraction of the ambient fluid, and λ_0 the wave length in vacuum of the laser light. A directional measurement is provided by the use of a Bragg cell. The signal produced by the vibrometer is demodulated by a *Dantec* 55N21 frequency tracker. The analogue output voltage of the tracker depends linearly on the target velocity. After subtraction of the offset which is related to the selected preshift frequency, the relative position is found by integration of the signal.

Measurements have been taken in the plane of symmetry of the sheet pipes perpendicular to the flow direction. The vessel surrounding the film pipe is connected to the test pipe in a point 0.95 m downstream.

The histograms of relative positions for various Reynolds numbers are given in Fig. 3. It is observed that for $Re_D \leqslant$ 200000 the width of the histograms increases only slightly with the flow, whereas above this Reynolds number it increases rapidly. Most histograms feature two maxima, which is an indication of a strong harmonic component in the motion. Since part of the motion of the film pipes may be caused by vibrations in the test-rig, we also conducted measurements of the displacement of a rigid part of the measurement section between two optical boxes.

The amplitudes of both the motions of the film pipe and the motion of the test rig at several Reynolds numbers are shown in Fig. 4. The amplitude is defined as the difference between the minimum and the maximum values in the position-histograms such as shown in Fig. 3. Figure 4 reveals, that for Reynolds numbers until 150000 the motion of the film pipes cannot be separated from the motion of the test-rig as a whole. Only for Reynolds numbers of 200000 and larger the motion of the film pipe is significantly larger than that of the test-rig, the maximum histogram width being 200 μm for $Re_D = 300000$. Also given in Fig. 4 is the relation between Re_D and the size of the often used wall unit ν/u_τ, with ν the kinematic viscosity and u_τ related to the wall friction τ and the density ρ as $\tau = \rho u_\tau^2$.

A more complete description of the dynamics of the motion can be obtained by spectral analysis of the vibrometer signal. Figure 5 shows power spectra of the velocity signal obtained from the film pipes for six Reynolds numbers. At two Reynolds numbers, the spectrum of the velocity signal of a rigid part of the test section is obtained. We call this the "background motion". For $Re_D = 50000$, the largest fluctuations in the velocity of the film pipes occur in a frequency range between 10 and 20 Hz. This motion is almost entirely imposed by background motion, which can be seen by comparison of the spectrum of the film pipe motion and the corresponding spectrum of the rigid part. For the next and higher Reynolds numbers, spectral components appear at higher frequencies than the background motion. Note that these spectra concern the velocity fluctuations of the film pipe rather than the position fluctuations. Since the position signal is the integrated velocity signal, the strong high-frequency peaks in the power spectra for $Re_D = 100000$, 150000 and even 200000 represent relatively weak increases of the relative displacement of the film pipe wall. For $Re_D \geqslant 200000$ the motion of the film pipe itself is dominant, the power being more and more concentrated around 200 Hz. The increasingly harmonic character of the pipe wall motion can also be observed from the position histograms in Fig. 3: the probability density function of a sinusoidal function exhibits maxima at the extrema of the oscillation, separated by a local minimum. The histograms for $Re_D = 250000$ and 300000 have these features. The shape of these histograms suggests a harmonic motion superposed on a more random-like motion. Note that the oscillation

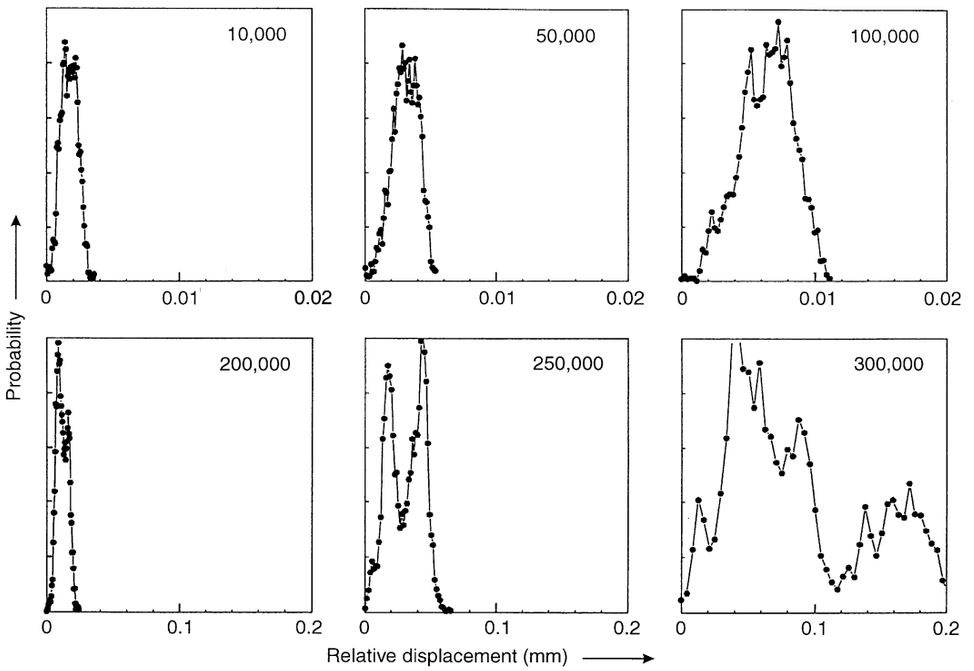

Fig. 3. Histograms of the relative position of the flexible pipe wall, for various Reynolds numbers. Note the difference between the horizontal scales of the upper and lower row

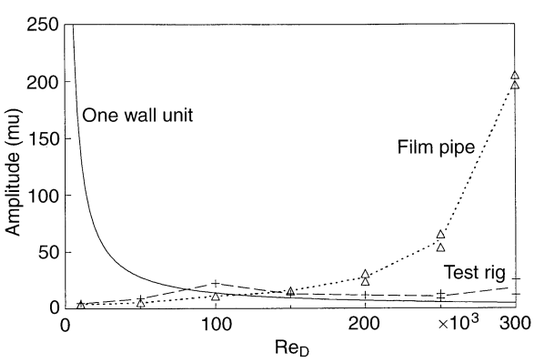

Fig. 4. Amplitudes (position histogram widths) of the motion of the film pipe (△) and of the test rig (+), for various Reynolds numbers

frequency of the film pipes is independent from the time scale related to the flow rate in the pipe. This implies, that the motion of the film pipes is not directly driven by the pressure fluctuations related to the large eddies in the flow, but rather exhibits a resonance-like behaviour.

For the application of the optical measurement section the film pipe motion has two consequences:

1. the position of the optical interface is time-dependent, and
2. the flow itself is slightly disturbed.

As we will see later, the amount of refraction to be expected with thin walls is so small, that the modulation of the refraction due to film pipe motions is negligible. The second effect, the disturbance of the flow, consists of two parts:

1. a direct displacement of the boundary layer, which becomes unsteady and slightly curved, and
2. an indirect global effect, viz. the acceleration of the flow due to an instantaneous change of the pipe's cross section.

The measured displacements rule out this second effect. The importance of the first effect depends on how far from the wall the oscillation is sensed. A position fluctuation with an amplitude of 100 μm and a frequency of 200 Hz generates a maximum wall velocity of 0.12 m/s, which is not small compared to the typical radial velocity fluctuations in turbulent pipe flows at $Re_D = 300000$. Also the wall displacements may induce some uncertainty in the exact position of the probe volume, when expressed in viscous wall units as defined above. Whether or not this is acceptable depends on the experimental technique applied.

5
Refraction by film-manufactured pipes

It is our aim to investigate the refractive effect of pipes made out of transparent film. First, we will discuss the optical properties of transparent films, and their recognition in practice.

5.1
Birefringence

Many commercially available transparent films exhibit birefringence, i.e. the phase velocity of light waves within the material depends on the direction of polarization with respect to the so-called optical axis. Figure 6 gives a cross-sectional view on the film, with the optical axis *o.a.* perpendicular to the

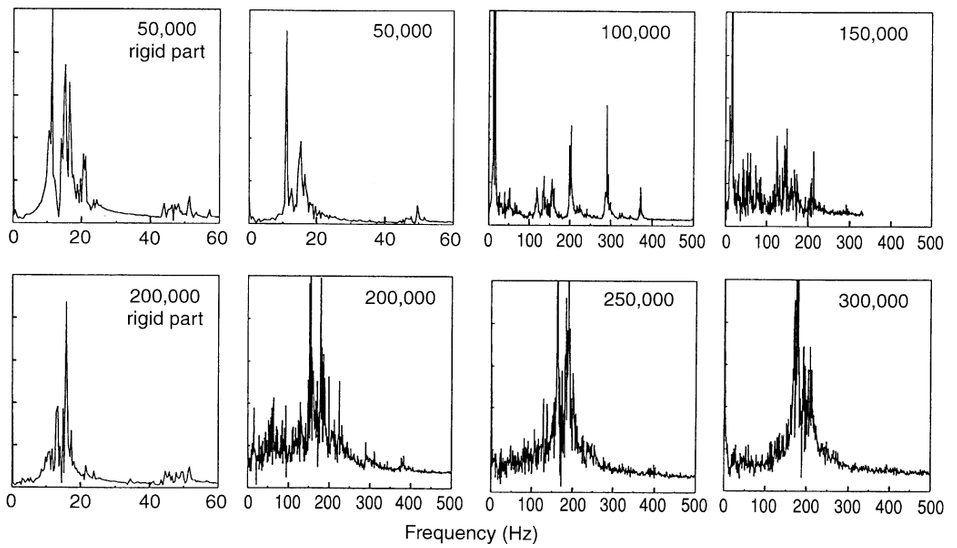

Fig. 5. Power spectra of the velocity signal of the vibrometer, for various Reynolds numbers

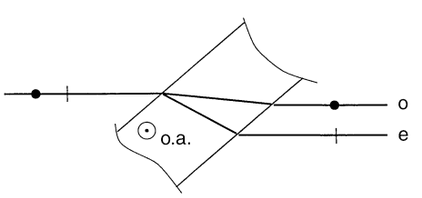

Fig. 6. Propagation of a light beam through birefringent material

plane of view. A beam of light enters the film at an angle of incidence α. Since the index of refraction of the polarization component in the direction of the *o.a.* differs from the perpendicular component, the beam will be split up into two linearly polarized beams, the so-called *ordinary* beam (denoted by "o" in Fig. 6) and *extraordinary beam* ("e"). Although in the geometry of Fig. 6 no splitting occurs at orthogonal incidence, yet the state of polarization of the beam will be modified. It is obvious, that birefringence is particularly important for laser-Doppler anemometry, since the processes of light scattering and photodetection depend on the state of polarization. Furthermore, the splitting of the beams may yield erroneous results.

5.2
Recognition of birefringence, and determination of the optical axis

Birefringence is easily recognized by means of a polariscope, which is a combination of two rotatable sheet polarizers. The film is illuminated by a monochromatic light source through the first polarizer whose transmission axis is aligned horizontally, and observed through the second polarizer adjusted perpendicular to the first polarizer. Since the state of polarization of light entering the film is altered depending on the direction of the optical axis, the amount of light passing the second polarizer will change when the film is rotated about the system axis of the polariscope.

During a complete rotation of the film, its appearance will be dark in four angular positions. These angular positions must be perpendicular to each other. In each of these angular orientations, the film pipe may be rotated about its vertical axis. In two orientations (differing by 180°) the film will remain dark, while in the two other cases light will be observed through the film. When the film remains dark, the optical axis of the film is in the vertical position, and hence is known.

5.3
Determination of the refractive indices of birefringent film

The refractive indices of birefringent polyester film with a thickness of 85 μm are determined with the aid of an interferometer. When a light beam traverses through the film, its optical path length is changed when the angle of incidence between the plane of the film and the beam direction is altered. This phase change may be observed when the film is included in one branch of an interferometer.

The interferometer is shown in Fig. 7 (*bottom*), and consists of a laser L, a beam splitter BS, a compensator C, a beam recombiner BR, mirrors M, a polarizing filter P and a screen S on which the fringe pattern is made visible. The investigated film F can be rotated about an axis perpendicular to the incoming laser beam. In Fig. 7 (*top left*) the light beam hits the film perpendicularly. When the beam travels a distance x_2, its optical path length is

$$\Lambda = x_2 + d(n-1) \tag{2}$$

with n the refractive index to be determined. In Fig. 7 (*top right*), the film has been rotated by an angle γ. Now the length of the trajectory of the beam through the film is

$$D = d/\cos\alpha \tag{3}$$

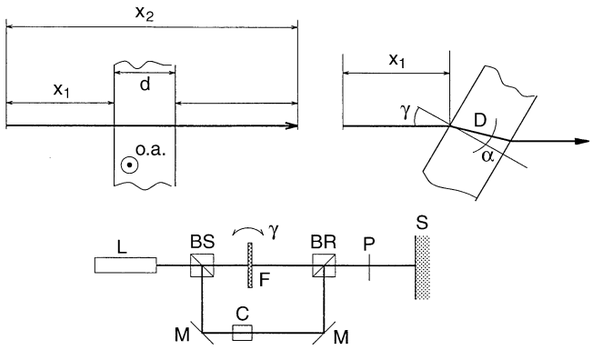

Fig. 7. Determination of refractive index of a thin film. *Bottom*: setup of the interferometer; *Top*: Rays passing through the transparent film F

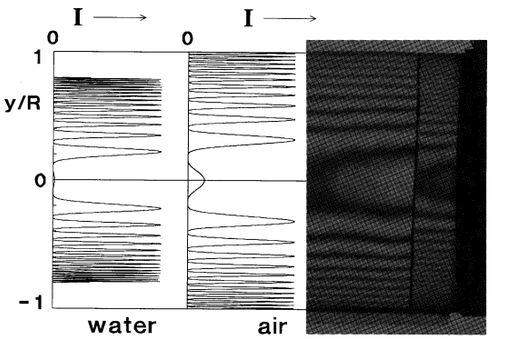

Fig. 8. Changes in polarization of light traveling through a cylindrical wall made of polyester sheet; *Left*: calculated. *Right*: viewed through a polariscope (in air)

with

$$\alpha = \arcsin(\sin\gamma/n) \tag{4}$$

Hence, the optical path length is

$$\Lambda = x_2 + nD - D\cos(\gamma - \alpha) \tag{5}$$

This can be rewritten as

$$\Lambda = x_2 + d\left[\frac{n-(\sin^2\gamma/n)}{\cos\{\arcsin(\sin\gamma/n)\}} - \cos\gamma\right] \tag{6}$$

When the film is placed in one branch of the interferometer, a rotation of the film results in a translation of the fringe pattern. Suppose that during a shift of the film between γ_1 and γ_2, the fringe pattern has shifted over N fringes. Then the optical path length has changed by an amount

$$\Delta\Lambda = |\Lambda_2 - \Lambda_1| = N\lambda \tag{7}$$

with λ the wavelength of light in vacuum. We can determine the index of refraction n by defining the function

$$F(n) = \left|\frac{n-(\sin^2\gamma_2/n)}{\cos\{\arcsin(\sin\gamma_2/n)\}} - \frac{n-(\sin^2\gamma_1/n)}{\cos\{\arcsin(\sin\gamma_1/n)\}} - \cos\gamma_2 + \cos\gamma_1\right| \tag{8}$$

This is an implicit function for refractive index n. For given values of γ_1, γ_2, N and λ, the refractive index of the film is the value of n for which

$$F(n) = N\lambda/d \tag{9}$$

This condition follows after substitution of Eq. (6) in Eq. (7).

To apply this method to birefringent material, the axis of rotation of the film should coincide with the direction of the optical axis *o.a.*, as indicated in Fig. 7 (*top left*). To obtain n_o, the *o*-ray should be selected. This is achieved by adjusting the polarizing filter P such that it transmits light polarized into the direction of the optical axis. When P is adjusted perpendicularly to this direction, n_e is obtained.

With the method described above, we have found the following values to hold for a 85 μm polyester film: $n_o = 1.27$ and $n_e = 1.47$. Since the refractive index of water has a value of 1.33, the ordinary rays will be refracted in a manner opposite to the extraordinary rays.

5.4 Consequences of birefringence

When a linearly polarized laser is used, and the user is free to adjust the plane of polarization, the effect of birefringence may be avoided: choose the orientation of the optical axis such that it is parallel to the axis of the pipe. When furthermore the direction of polarization of laser light that enters the measurement section is chosen either vertically or horizontally, the state of polarization of the beams will not be altered by the pipe wall. In some LDV systems, however, a rotation of the polarization of the laser light will change the effect of beam splitters and mirrors, which may lead to undesirable changes in the intensity of the crossing beams.

A typical example of the change of the state of polarization is shown in Fig. 8 (*right*). A film pipe whose front half has been cut away is illuminated by linearly polarized red light under an angle of 45° to the pipe axis. The optical axis of the polyester film is almost parallel to this axis of symmetry of the pipe. The photograph was taken through a polarizing filter transmitting light which is polarized in the same direction as the incoming light. We observe dark and bright bands, approximately parallel to the axis of the pipe. The centres of the dark bands indicate locations in which the polarization is linear and has an angle of 90° with respect to the original direction, while in the centres of the bright bands the light is linearly polarized in the original direction. In the regions in between, the light is elliptically polarized, which is observed when one of the polarizers is rotated by 90°: the light bands become dark and vice-versa, without changing position. The width of the bands decreases with increasing distance from the pipe centre, where the optical path length through the film increases. It can be shown that when the incoming light is polarized under an angle of 45° with the optical axis, the

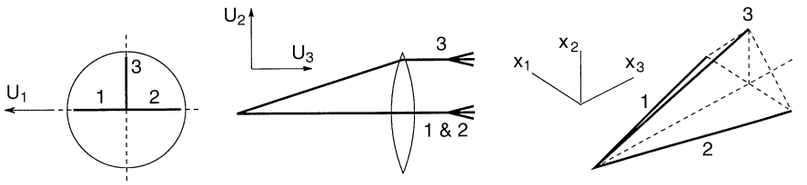

Fig. 9. Definition of beam indices and velocity components U_k, $k=1, 2, 3$ in a coordinate system fixed to the LDV system. Transmitting lens and laser beams are seen in front view (*left*), side view (*middle*) and in perspective (*right*)

intensity of the observed light behaves like

$$I\left(\frac{y}{R}\right)=\frac{1}{4}\mathrm{I}_{\max}\left[1+\cos\frac{2\pi}{\lambda}\left|\Lambda_e-\Lambda_o\right)\right|\Bigg]^2 \tag{10}$$

with the optical path length difference of the *e*- and *o*-ray

$$\left|\Lambda_e-\Lambda_o\right|=d\left|\sqrt{\left(\frac{n_e}{n_a}\right)^2-\left(\frac{y}{R}\right)^2}-\sqrt{\left(\frac{n_o}{n_a}\right)^2-\left(\frac{y}{R}\right)^2}\right| \tag{11}$$

with n_a the index of refraction of the ambient medium. Equations (10) and (11) are valid when the curvature of the pipe wall may be neglected, while also the reflection has not been taken into account. The calculated intensity is shown in Fig. 8 (*left*), for water and air as surrounding media. The results for air are more or less in agreement with the pattern shown on the photograph. In water the polarization-modifying effect is stronger than in air, due to the smaller local wave length λ, see Eq. (10).

The consequence for LDV is that the polarization of two initially parallelly polarized beams that enter the pipe at different y/R positions is changed by a different amount. This reduces the level of the photodetector signal, or using the fringe model for LDV, reduces the visibility of the fringes since two beams only interfere by their parallel components of the electric field.

5.5
Refractive deflection of laser beams

The above only accounts for the change of the state of polarization of the incoming beams. As pointed out earlier, birefringence also causes the beam to split, which cannot be observed on the light screen used for Fig. 8.

Since this splitting is caused by different amounts of deflection of the *e*-beam and the *o*-beam, we will assess this effect from the results of a normal refraction calculation. Here we will consider the specific case of laser-Doppler measurements of two velocity components. The LDV-system is operated in the reference beam mode. The beam configuration is shown in Fig. 9, along with the definition of the velocity components. Beam 3 provides the light to be scattered, while beams 1 and 2 act as reference beams. The nominally measured velocity components are those perpendicular to the system axis, *viz.* U_1 and U_2.

The effect of refraction on the beam configuration is shown in an exaggerated way in Fig. 10. The undistorted beams (the dashed lines) intersect each other in point P. In this figure, it is shown that

1. The plane of the reference beams 1 and 2 is tilted in the vertical direction, resulting in displacement of the point of intersection of these beams from P to P′. The distance between P and P′ is denoted by Δy in the horizontal direction, and Δz in the vertical direction.
2. The scattering beam 3 has undergone a different amount of refraction, as a result of which beam 3 does not intersect the other beams. Beam 3 intersects the plane of the other beams in point P″.

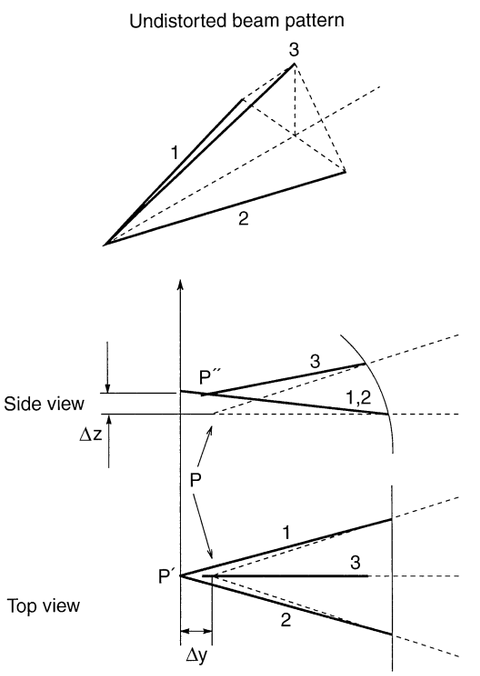

Fig. 10. Distortion of the beam configuration by refraction in a cylindrical wall. Beams *1* and *2*: reference beams, beam *3*: scattering beam. Dashed lines: unrefracted beams. Bold lines: refracted beams

The tilt of the reference beams induces a similar tilt of the coherence cones around these beams. Furthermore, the scattering beam does not intersect the axis of symmetry of these cones, due to which the vector describing the mean direction of the scattered light that interferes with the reference beam does not coincide with the reference beam vector.
The final result is

1. a reduction of the signal amplitude;
2. a change in the system's response to the velocity vector, and
3. a difference between the real measurement location and the nominal location.

Using Snell's law, calculations have been performed of the distortion of the laser beam configuration, as a function of the undistorted position of the measurement volume in the LDV

measurement section. The undistorted beam pattern is the one depicted in Fig. 9 with an angle of 8° between the beams *in air* and the system axis. The cylindrical wall has a thickness of 87 μm and an index of refraction of 1.47. The following quantities have been calculated:

- the displacements Δy and Δz of the intersection point of the reference beams 1 and 2;
- the smallest distance Δ_b between the scattering beam 3 and one of the reference beams;
- The angle ξ between the direction of the measured velocity component $\tilde{U}_2$ and U_2 into the direction of the x_2-axis, as defined in Fig. 9;
- The quantities α_1 and α_2 in the relations

$$\tilde{U}_1 = (1+\alpha_1)\,U_1 \quad \text{and} \quad \tilde{U}_2 = (1+\alpha_2)\,U_2 + \xi(1+\alpha_2)\,U_3 \qquad (12)$$

with the tilde denoting the really measured quantities.

Calculations have been performed in the domain limited by $0 \leqslant \phi \leqslant 2\pi$ and $0 \leqslant r/R \leqslant 0.986$. The polar angle ϕ is measured with relative to the x_3 axis, in the counter clockwise direction. The results are shown in Fig. 11. In spite of the asymmetry of the situation, the results are almost symmetric (or antisymmetric) with respect to the line $\phi = \pi$. The raggedness of the results for Δy is caused by the finite numerical accuracy of the computation. The results for α_1 are dominated by numerical "noise" within the range $|\alpha_1| < 4 \times 10^{-7}$, and have been omitted.

For the evaluation of our experiments, the subdomains $\phi \leqslant \pi/4$, $3\pi/4 \leqslant \phi \leqslant 5\pi/4$, and $7\pi/4 \leqslant \phi \leqslant 2\pi$ are most relevant. In these subdomains, the following extreme values are found:

- Maximum displacements of $\Delta y = 2$ μm and $\Delta z = 5$ μm, see Fig. 11a and b. These displacements are not significant compared to the accuracy of 0.1 mm to which the centre of the pipe can be localized.
- A maximum smallest distance between the reference beams and the scattering beam of $\Delta_b = 20$ μm, see Fig. 11c. This will hardly result in a signal deterioration both in the reference beam mode and in the dual beam mode, since the beams have a waist diameter of 100 μm.
- A maximum value of $\alpha_2 = 0.001$, see Fig. 11d. This results in an error in U_2 which is smaller than that associated with the theodolite calibration and the positioning inaccuracy.
- A maximum value of $\xi = 0.0002$ rad $= 0.01°$, see Fig. 11e. This rotation angle of the effectively measured velocity component U_2 is negligible.

If we would have taken an index of refraction of the pipe wall of $n = 1.27$, the results would have been oppositely signed, and a factor 4 smaller. Our conclusions about the negligibility of refraction effects still hold, if our results are compared with those that would have been obtained for $n = 1.27$ rather than with the undistorted case.

Even on vertical traverses, $\phi = \pi/2$ until close to the wall, beam refraction will not cause serious errors, compared to the other sources of error.

The negligibility of refraction effects also holds for the beam splitting property that is inherent to birefringence. Within the above mentioned subdomain, the two resulting beams will have undergone a mutual displacement in the order of 10 μm, which is acceptable compared to the beam waist diameter.

6 Selection of film type

A question to be addressed finally is, which type of film should be prefered. The answer depends, of course, on the

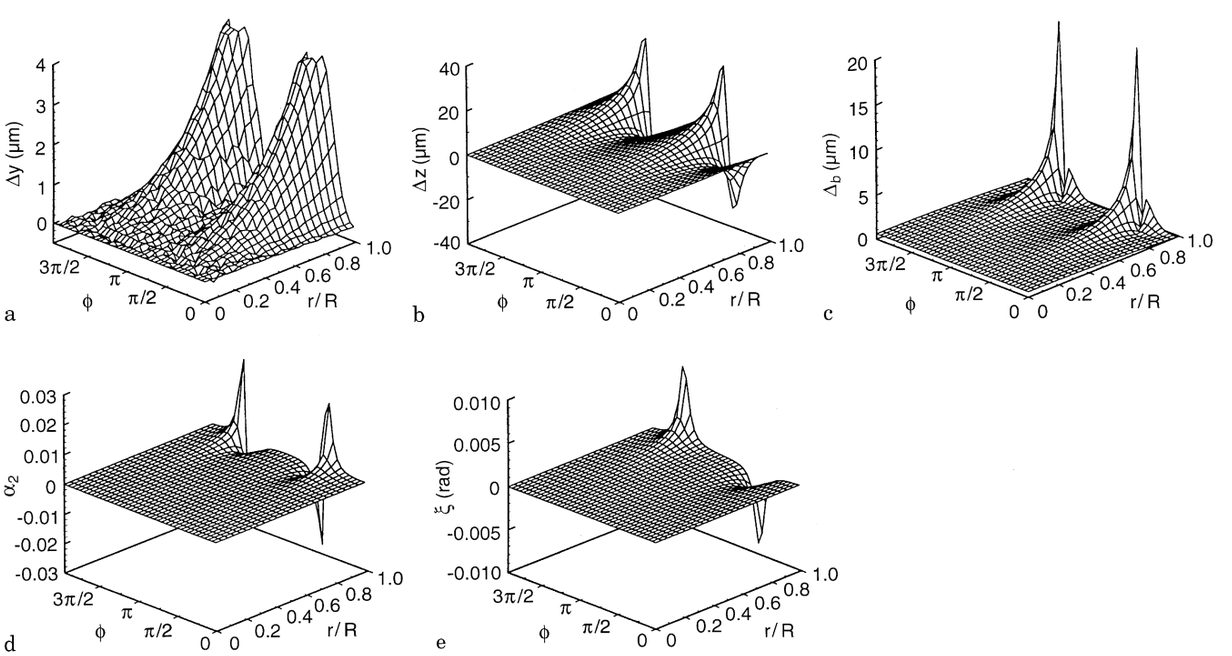

Fig. 11a–e. Calculated distortion by refraction of the laser beam configuration

application at hand, and general recommendations can hardly be given. The ideal film is non-birefringent, has an index of refraction close to that of the working fluid, is perfectly smooth and homogeneous, and does not absorb the working fluid. In practice there is no film possessing all these properties. Here some practical experiences will be given.

Water absorption The temporal neglect of this aspect has caused the author some trouble. Water absorption causes film expansion, due to which the film pipe may buckle. An extremely high absorption was found for some type of acetate-film, which directly deforms after wetting one side.

Refraction/birefringence Birefringence was observed in films made of polyester and of PVC, and was not observed in polycarbonate film and PTFE-FEP film. Our calculations show that for most measurements the index of refraction is hardly important for film thicknesses below 100 μm. Particularly interesting for use in water is film made of a PTFE-FEP copolymer, which has a refractive index of 1.34–1.35. A disadvantage of this film is its resistance against adhesive materials.

Brightness and smoothness Some seemingly smooth and clear films feature, at a closer look, small scale optical inhomogeneities. The smoothest and clearest film found by the author was polyester film. The film actually used in this study was an anonymous standard overhead transparency made of polyester.

7 Conclusions

In this article we have described an optical measurement section for the investigation of liquid flows through straight pipes. In this measurement section, the pipe wall is made from a thin, flexible, transparent sheet with a thickness of 85 μm. The cylindrical sheet is surrounded by a rectangular box filled with fluid, which is kept at a slight underpressure. Interferometric measurements have been performed of the movements of the flexible pipe wall due to turbulent pressure fluctuations. Until a Reynolds number $Re_D = 150000$ the movements cannot be discerned from those made by the entire test rig. Above this Reynolds number the amplitude of the motion increases rapidly, to obtain a value of 200 μm (top-top value) at $Re_D = 300000$. No artifacts of this movement were found in the results of laser-Doppler measurements along a horizontal axis.

Some thin transparent sheets exhibit strong birefringence. The effect on the polarization of a linearly polarized laser beam may be minimized by matching the optical axis of the film and the direction of polarization. For a pipe wall of the present thickness, the effect of refraction was shown to be negligible, and no additional correction is needed in laser-Doppler measurements. The same conclusion holds for the beam-splitting effect of birefringence.

References

Boadway JD; Karahan E (1981) Correction of laser doppler anemometer readings for refraction at cylindrical interfaces. DISA Information 26: 4–6

Buchhave P (1975) Laser doppler vibration measurements using variable frequency shift. DISA Information 18: 15–20

Dybbs A; Edwards RV (1987) Refractive index matching for difficult situations, in: Laser anemometry: advances and applications. In: Proceedings of the Second International Conference on Laser Anemometry, Advances and Applications. 1–22

Hinze J (1975) Turbulence, 2nd Edition, McGraw-Hill

Kunen J (1984) On the detection of coherent structures in turbulent flows. Ph.D. Thesis, Delft University of Technology, the Netherlands, Laboratory for Aero and Hydrodynamics

Lowe ML; Kutt PH (1992) Refraction through cylindrical tubes. Exp Fluids 13: 315–320

Maanen HRE Van; Fortuin JMH (1983) Experimental determination of the random lump-age distribution in the boundary layer of the turbulent pipe flow using laser doppler anemometry. Chem Eng Sci 38: 399–423

Mizushina T; Usui H (1977) Reduction of eddy diffusion for momentum and heat in viscoelastic fluid flow in a circular tube. Phys Fluids 20: S100–S108

Ritterbach E; Hoettges J; Els H (1987) Optical improvement of LDV-measurement in pipe flow. In: Laser anemometry: advances and applications. Proceedings of the Second International Conference on Laser Anemometry, Advances and Applications. 299–311.

Schlichting H (1979) Boundary Layer Theory, 7th Edition, McGraw-Hill